

# An extraordinary tabletop speed of light apparatus

Guido Pegna

Citation: *American Journal of Physics* **85**, 712 (2017); doi: 10.1119/1.4985728

View online: <http://dx.doi.org/10.1119/1.4985728>

View Table of Contents: <http://aapt.scitation.org/toc/ajp/85/9>

Published by the [American Association of Physics Teachers](http://www.aapt.org)

---

---



American Association of **Physics Teachers**

Explore the **AAPT Career Center** – access hundreds of physics education and other STEM teaching jobs at two-year and four-year colleges and universities.

<http://jobs.aapt.org>



# APPARATUS AND DEMONSTRATION NOTES

The downloaded PDF for any Note in this section contains all the Notes in this section.

John Essick, *Editor*

*Department of Physics, Reed College, Portland, OR 97202*

This department welcomes brief communications reporting new demonstrations, laboratory equipment, techniques, or materials of interest to teachers of physics. Notes on new applications of older apparatus, measurements supplementing data supplied by manufacturers, information which, while not new, is not generally known, procurement information, and news about apparatus under development may be suitable for publication in this section. Neither the *American Journal of Physics* nor the Editors assume responsibility for the correctness of the information presented.

Manuscripts should be submitted using the web-based system that can be accessed via the *American Journal of Physics* home page, <http://ajp.dickinson.edu> and will be forwarded to the ADN editor for consideration.

---

## An extraordinary tabletop speed of light apparatus

Guido Pegna<sup>a)</sup>

*Department of Physics, University of Cagliari, Città Universitaria, 09042 Monserrato, Italy*

(Received 11 April 2012; accepted 30 May 2017)

A compact, low-cost, pre-aligned apparatus of the modulation type is described. The apparatus allows accurate determination of the speed of light in free propagation with an accuracy on the order of one part in  $10^4$ . Due to the 433.92 MHz radio frequency (rf) modulation of its laser diode, determination of the speed of light is possible within a sub-meter measuring base and in small volumes (some  $\text{cm}^3$ ) of transparent solids or liquids. No oscilloscope is necessary, while the required function generators, power supplies, and optical components are incorporated into the design of the apparatus and its receiver can slide along the optical bench while maintaining alignment with the laser beam. Measurement of the velocity factor of coaxial cables is also easily performed. The apparatus detects the phase difference between the rf modulation of the laser diode by further modulating the rf signal with an audio frequency signal; the phase difference between these signals is then observed as the loudness of the audio signal. In this way, the positions at which the minima of the audio signal are found determine where the rf signals are completely out of phase. This phase detection method yields a much increased sensitivity with respect to the display of coincidence of two signals of questionable arrival time and somewhat distorted shape on an oscilloscope. The displaying technique is also particularly suitable for large audiences as well as in unattended exhibits in museums and science centers. In addition, the apparatus can be set up in less than one minute. © 2017 American Association of Physics Teachers.

[<http://dx.doi.org/10.1119/1.4985728>]

### I. INTRODUCTION

The speed of light  $c$  is perhaps the most important fundamental constant in physics. Since October 21, 1983, it is a primary standard of measurement, on which the new definition of the meter depends. The extraordinary high value of  $c$  makes its determination in instructional laboratories an attractive challenge.

Judging from the large number of papers that have been published in this journal, the methods for the determination of  $c$  in free propagation are of great interest. These different approaches can be classified into four categories: modulation methods;<sup>1–4</sup> pulse methods for the measure of time of flight,<sup>5–11</sup> with the special category of pulse methods that use the structure of longitudinal modes of laser cavities;<sup>12–14</sup> new versions of classical methods such as Foucault's rotating mirror;<sup>15,16</sup> and finally methods that rely on interference effects or electrical pulses. This last category includes, for instance, the propagation time of electrical pulses in coaxial cables,<sup>17,18</sup> the interference of microwaves,<sup>19</sup> electromagnetic waves generated by a microwave

oven by measuring the length of the modes in the cavity or extracting some energy and using Lecher lines,<sup>20</sup> the reflection of TV radio waves by distant obstacles,<sup>21–23</sup> and even the time of propagation of Ethernet packets in a cable connecting two computers.<sup>24</sup>

In modulation methods, the intensity of the light source is sinusoidally modulated and the phase of the signal received at a certain distance is compared to that of the modulating signal. In all the published papers noted above, this comparison is performed by displaying the signals on the screen of an oscilloscope. Owing to inevitable distortion in the processes of modulation, detection, and amplification, this comparison is significantly affected by uncertainty, even when using Lissajous figures.

The innovative idea at the heart of our design is this: a light signal is modulated at a radio frequency (rf) and delayed with respect to a reference signal at the same frequency. The delay, due to a certain distance traveled by the light, creates a phase shift between the modulated light signal and the reference signal. Instead of displaying this phase

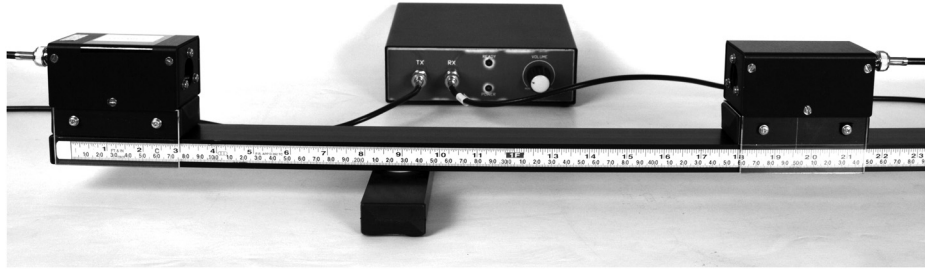


Fig. 1. The complete apparatus, ready to operate, including the transmitting unit (left), the receiving unit (right), and the control module (middle).

shift on an oscilloscope, the two signals are further modulated using an audio frequency signal. When the two (twice modulated) signals are recombined, their phase difference is “displayed” as the loudness of an audio signal. The experimenter can find the points at which the signals are completely out of phase by varying the delay of the light signal to minimize the loudness of the audio signal. Finding two adjacent minima yields a measurement of the half wavelength of the rf modulation signal. Since one knows the frequency, one can compute the speed of light.

In this instrument, the source is a collimated red laser diode. The modulation frequency of 433.92 MHz is, to our knowledge, by far the highest among those that appear in the literature and in commercial apparatuses. As a consequence, the measuring base is reduced to only  $c/2f \sim 0.35$  m—the shortest among those reported—and from that derives the compactness of the whole apparatus. The optical bench is only 1.5 m long, so it may lie on a normal table and is easily transportable. The very high modulation frequency also allows insertion of transparent objects of small thickness into the laser beam for the determination of their refraction index. This technique is so sensitive that the slowing of light through the thickness of a microscope slide can be detected!

The apparatus, as shown in Fig. 1, is composed of a transmitting unit, positioned at one end of the optical rail; a receiving unit that slides along the rail; and a control, display, and power supply module that is connected to the transmitter and receiver. Given the limited length of the measuring base, the sliding receiver remains aligned with the laser beam, eliminating any need for preliminary alignment. The apparatus as shown in Fig. 1 is complete and autonomous. Other components, such as an oscilloscope, power supply, optical rails, lenses, or mounting holders, are not needed, nor are other expensive components such as photomultipliers, electro-optic modulators, external cavity lasers, and scanning Fabry-Perot interferometers. Set up of the apparatus requires less than a minute, the delicate and time-consuming installations and alignments usually required by other speed-of-light apparatuses being unnecessary.

## II. THE SYSTEM

The mechanisms of modulation, demodulation, and extraction of the audio signal are illustrated in elementary terms as follows. The general structure of a modulation-demodulation system is shown in Fig. 2. When a laser diode is modulated by variation of its injection current, the resulting optical carrier is mainly amplitude modulated. Let  $p(t) = P \cos(\omega_p t)$  be the optical carrier of angular frequency  $\omega_p \approx 2\pi(4 \times 10^{14})$  rad/s and  $m(t) = A + M \cos(\omega_m t)$  be the modulating signal of angular frequency  $\omega_m \approx 2\pi(433.92 \times 10^6)$  rad/s. For now, the

phase shift of the modulation (relative to the carrier) signal is not indicated for simplicity. The process of modulation of the laser is equivalent to the product of  $p(t)$  and  $m(t)$

$$\begin{aligned} y(t) &= [A + M \cos(\omega_m t)]P \cos(\omega_p t) \\ &= AP \cos(\omega_p t) + MP \cos(\omega_m t) \cos(\omega_p t) \\ &= AP \cos(\omega_p t) + \frac{MP}{2} \\ &\quad \times [\cos(\omega_p + \omega_m)t + \cos(\omega_p - \omega_m)t], \end{aligned} \quad (1)$$

where we can see that the modulated optical carrier consists of an unmodulated optical component and two optical *sideband* components, the frequencies of which are shifted from that of the optical carrier by the modulating frequency (i.e., by  $\pm f_m$ ).

The ratio  $(A + M)/P$  is the *amplitude modulation index*, which is expressed in general as a percentage, and for modulation fidelity must be maintained below 100%, as we shall see later.

The photodiode is a square-law detector: its output is an electric signal that is proportional to the intensity of the optical signal it receives, which in turn is proportional to the square of the instantaneous optical amplitude. Squaring Eq. (1) and neglecting the resulting terms involving  $\omega_p$  and  $2\omega_p$  (because the photodiode cannot respond to these THz optical signals), we find the following relation for the photodiode’s electrical output:

$$E = \frac{1}{2}AMP^2 \cos(\omega_m t) + \frac{1}{8}M^2P^2 \cos(2\omega_m t). \quad (2)$$

The first term in this equation is proportional to the maximum amplitude  $M$  of the modulating rf signal, has the same frequency, and also carries the phase information. The second term is a small second-harmonic distortion signal, but in our experiment its amplitude will be even smaller than predicted here because of the much lower response of the photodiode at this higher frequency. We conclude that the output of a photodiode that receives an amplitude modulated light signal is an electrical signal proportional to the square of the

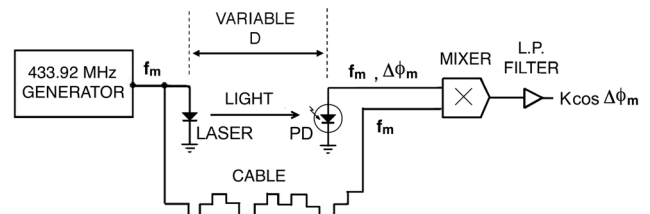


Fig. 2. The general principle of the modulation method.

maximum amplitude of the optical carrier with the frequency and phase of the modulating signal. Another way of expressing this result is the following: the output of a photodiode that receives an optical carrier signal modulated at high frequency is an electrical signal generated by the optical beats between the carrier and its sidebands.

We will now consider phase shifts and the phase recovery technique as illustrated in Fig. 2. First, we define

$$E_m = V_m \cos(\omega_m t + \varphi_m), \quad (3)$$

where  $V_m = AMP^2/2$  and phase information has been now included via the phase constant  $\varphi_m$ . In Fig. 2, the output voltage  $E_m$  of the photodiode of angular frequency  $\omega_m$  is sent to a balanced mixer. Let  $\Delta\varphi_m$  be the phase difference between  $E_m$  and the reference signal  $V_r$ , which is sent to the mixer by a cable. Then,  $\Delta\varphi_m$  is the sum of the initial phase  $\varphi_m$  and the added phase rotation due to the travel of light from the source to the photodiode. The mixer output is the product of these signals

$$\begin{aligned} V_{\text{out}} &= V_m V_r \cos(\omega_m t + \Delta\varphi_m) \cos(\omega_m t) \\ &= \frac{1}{2} V_m V_r [\cos \Delta\varphi_m + \cos(2\omega_m t + \Delta\varphi_m)]. \end{aligned} \quad (4)$$

In our circuit, the signal at twice the rf modulating frequency ( $2\omega_m$ ) is eliminated by a low-pass filter. The remaining signal,

$$V'_{\text{out}} = \frac{1}{2} V_m V_r \cos \Delta\varphi_m, \quad (5)$$

is a dc voltage proportional to the cosine of the phase difference between the two signals. This phase difference contains the time delay of the light in its travel through air.

### III. DETERMINATION OF THE SPEED OF LIGHT

The rf generator in Fig. 2 is amplitude-modulated by a square wave, so that its rf output signal (and consequently the envelope of the light emitted by the laser) varies from zero to its normal rf amplitude according to this square-wave signal. The square wave has frequency  $f_a$  in the audio range as indicated in Fig. 3. Thus, at the output of the system, instead of the dc signal  $V'_{\text{out}}$  of Eq. (5), we will find a signal of frequency  $f_a$ , whose loudness will be zero when  $\Delta\varphi_m$  is  $\pi/2, 3\pi/2$ , etc.

Because this signal can be amplified at will, the sensitivity will be maximum if we use a null method of detection. To exploit this feature, we move the receiver along the rail to the positions for which the audio signal is minimal. These positions are those for which  $\Delta\varphi_m = \pi/2, 3/2\pi, \dots$  and thus correspond to distances  $D_n$  from the transmitter that satisfy

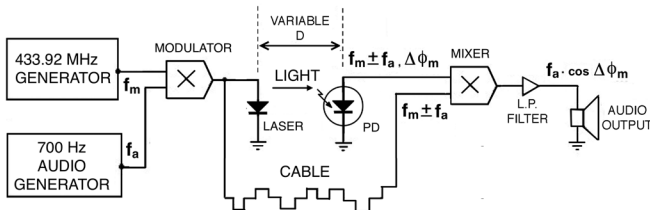


Fig. 3. The technique for displaying the phase coincidence audibly.

$$\Delta\varphi_m = 2\pi \frac{\tau}{T_m} = 2\pi \frac{f_m D_n}{c} = \frac{(2n+1)}{2} \pi, \quad (6)$$

where  $n = 0, 1, 2, \dots$ ,  $T_m = 1/f_m$  is the period of the rf modulating signal, and  $\tau$  is the propagation time of the light along the distance  $D_n$ .

Between the successive positions of the minima of the audio signal, the phase increases by  $\pi$ . The distance  $\Delta D_n = D_{n+1} - D_n$  between these minima is such that

$$2\pi \frac{f_m \Delta D_n}{c} = \pi, \quad (7)$$

from which we obtain

$$c = 2f_m \Delta D_n. \quad (8)$$

In reality, because of amplifier non-linearity, as well as possible overmodulation of the laser, the modulation envelope may not be perfectly sinusoidal. For example, Fig. 4 illustrates the distortion due to laser overmodulation. Because of this non-ideal behavior, there may be a difference in the distances between the positions of successive minima. To compensate for this defect, we look for the distance between every other minima, which corresponds to the propagation delay of a whole period  $T_m$  of the rf wave, thus modifying Eq. (8) to

$$c = f_m \Delta D, \quad (9)$$

with  $\Delta D = 2\Delta D_n$ .

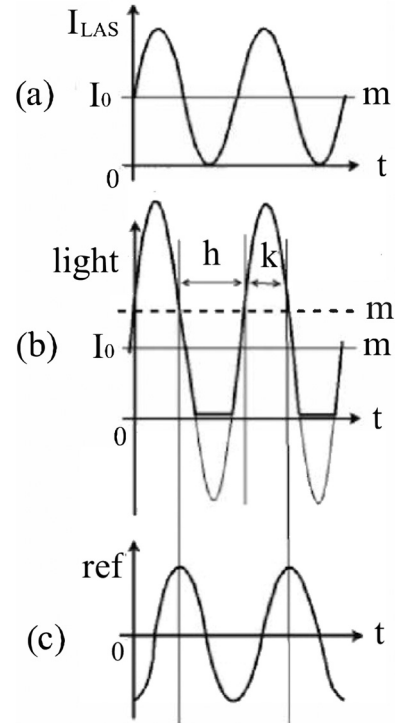


Fig. 4. (a) A graph showing 100% modulation of the laser current. Here,  $I_0$  is the bias current of 28 mA and  $m$  is the mean of the light emission. (b) A graph showing light emitted by a highly over-modulated laser. Here, the bias current is the same as in (a), but the mean of the light emission is shifted to  $m'$ . The resulting asymmetry between the two halves of the semi-period of modulation is evident. (c) A graph of the reference signal for the mixer. The figure shows that a good minimum is reached at only one position in each wavelength of the rf signal.

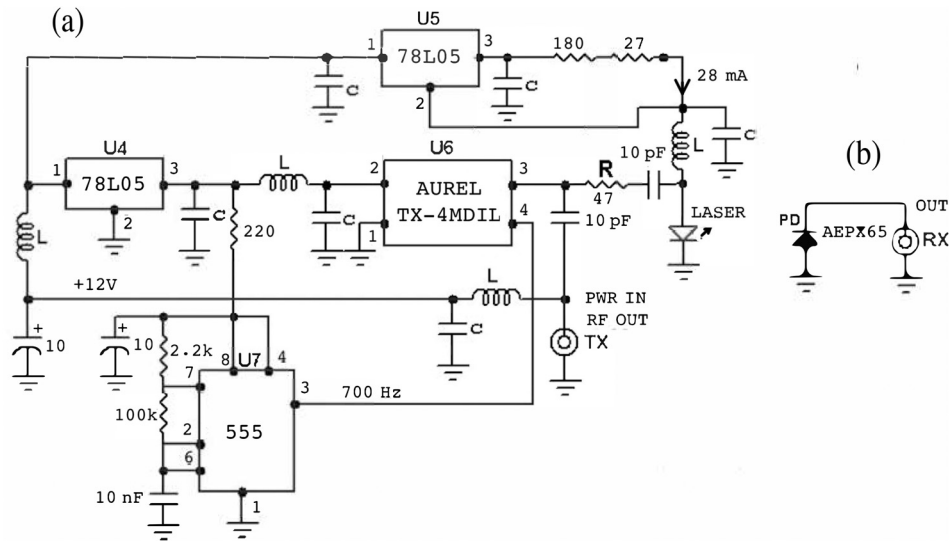


Fig. 5. Schematics diagrams of (a) the transmitter and (b) the receiver ( $C = 100$  nF and  $L = 100$  nH). When not indicated, capacitance is in microfarads and resistance in ohms. The cables to the TX and RX connectors feed both the input power supply and bias voltage, respectively, as well as the output rf signals.

#### IV. DESCRIPTION OF THE APPARATUS

The apparatus is shown in Fig. 1. The optical bench is made with an anodized aluminum rectangular profile of  $2 \times 4$  cm<sup>2</sup> cross section and a length of 150 cm. The transmitting unit is positioned at one end while the receiving unit can slide without lateral play, thus keeping its alignment with the laser beam. The control module supplies power to the transmitting and receiving units, detects the phase difference, and amplifies the audio signal. The two feet of the bench can be rotated by 90° for ease in transporting the apparatus. As seen in Fig. 1, the transmitting and receiving units are supported by a suitable length of the same rectangular cross section as the optical bench. Two rectangular pieces of acrylic are attached to these units to serve as sliding guides; on one side of the optical bench a scale graduated in centimeters and millimeters is attached, while on the corresponding acrylic guide of the receiving unit a thin vertical line is drawn as an index for reading the position of the receiver.

A schematic of the transmitter circuit is shown in Fig. 5(a). The rf generator and audio modulator is the integrated module U6,<sup>25</sup> whose output power of 1 dBm = 1.3 mW is more than adequate for modulating the laser. The modulator block shown in Fig. 3 as a separate component is actually integrated into U6, a digital data transmission module with a TTL level input control pin.

The modulation index of the light is adjusted to less than 1 by the choice of resistor  $R = 47 \Omega$  in Fig. 5(a). The value of this resistor determines the degree of equality of the various distances  $\Delta D$ , as explained above and in Fig. 4. The frequency of the module is stabilized by a Surface Acoustic Wave (SAW) device and remains stable to about one part in  $10^4$  after a warm-up time of ten minutes. This frequency can be measured with a frequency counter, which can be inserted by means of a BNC tee on the connector of the transmitting unit. The regulator U5 is wired as a constant current generator of 28 mA for the bias of the laser diode. The circuit U7 generates a square wave of about 700 Hz for the audio modulation of the radio frequency generator.

The laser diode with its collimator is obtained from an inexpensive class-II laser pointer, as shown in Fig. 6, which emits at approximately 650 nm. This component has been shown to operate reliably for years in our instructional laboratory. The interior of the transmitting unit is shown in Fig. 7; both the adjustment screws and the springs for alignment of the laser are visible in this photo.



Fig. 6. The laser pointer and its constituent components. The laser diode and collimator unit is at the lower right.

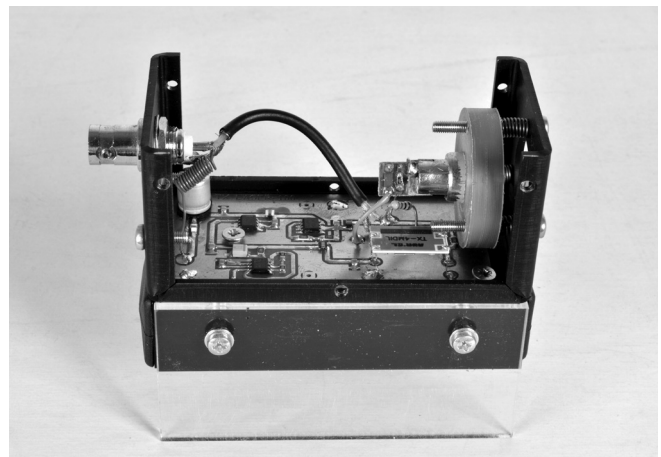


Fig. 7. The interior of the transmitter unit. The screws for beam alignment are visible. Surface mount integrated circuits are used. The transmitter module is visible on the lower right.

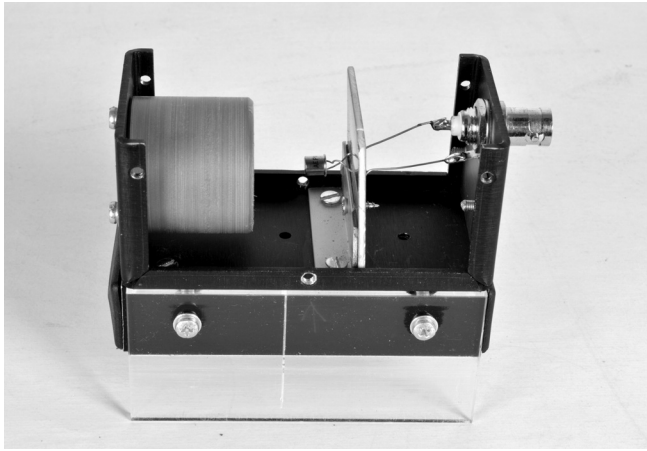


Fig. 8. The interior of the receiver unit.

Figure 5(b) shows the receiver circuit, consisting only of a photodiode, while Fig. 8 shows the interior of the receiving unit. A 20 mm-focal-length lens, whose main purpose is to compensate for any small lateral misalignment of the laser beam, acts to focus the light on the sensitive element of the photodiode. The photodiode, however, is positioned slightly away from the focus point of the lens. It is sometime useful to include inside the receiver a short length of 50  $\Omega$  coaxial cable between the photodiode cathode and the BNC output connector and to adjust its length by trial and error until the first minimum is located 1–2 cm from the transmitter. Such an adjustment allows one to take advantage of the entire length of the optical bench when measuring successive minima as the receiver is moved along the bench.

The AEPX65 photodiode,<sup>26</sup> which has a rise time of 1 ns and therefore a  $-3$  dB cutoff frequency of 0.35 GHz, is a good compromise between cost and performance; it works well at the modulation frequency of this apparatus.

The transmitter and receiver units are each connected to the control module with a single 50- $\Omega$ , RG58 cable terminated with a BNC connector. These cables carry the power supply for the transmitter and the bias voltage for the photodiode, and also carry back the rf signals to the control module. It is not necessary for the two cables to have the same length.

The control module circuit is shown in Fig. 9. Integrated circuit U1 is a balanced mixer that performs the phase comparison by determining the instantaneous product of the input signals. Only the audio signal is present at its output. An audio amplifier U2 and a power audio amplifier U3 follow. The connector marked OUT may be useful for viewing

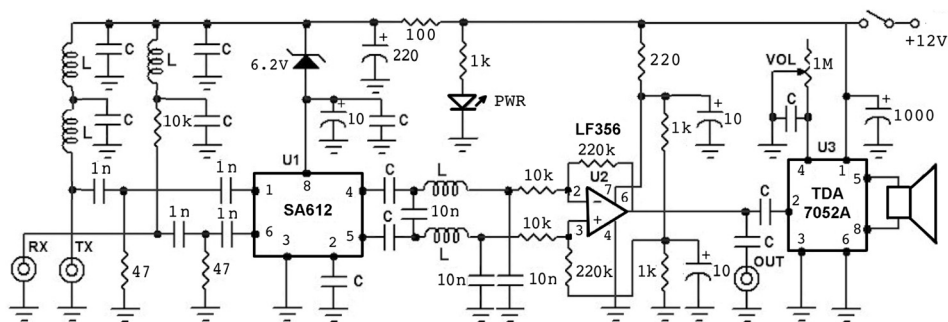


Fig. 9. Schematics of the control and display module ( $C = 100$  nF and  $L = 100$  nH). If not indicated, capacitance is in microfarads and resistance in ohms. Given the small power consumption, the apparatus can be independently powered by batteries.

the shape of the detected audio signal on an oscilloscope while adjusting the modulation depth of the laser, or to monitor the signal on an ac voltmeter. All of the inductors are small SMD (Surface Mount Device)<sup>28</sup> RF chokes of 100 nH inductance; they constitute a block for rf signals while allowing the dc components to pass. Figures 10 and 11 show relevant signals in various points of the system: the laser modulation waveform, the photodiode received signal and the detected signal in a zero position of the receiver.

## V. EXAMPLE EXPERIMENTS AND RESULTS

The installation of the apparatus consists of simply connecting the two cables from transmitter and receiver to the control box and inserting the plug into the power supply receptacle. After powering on and waiting a few minutes for the instrument to stabilize, the experiments are ready to perform.

### A. Determination of $c$

Starting with the receiver close to the transmitter, a search for a minimum in the audio signal is undertaken (adjustment of the audio level is helpful). The minimum of the audio signal is easily found by making small successive adjustments in the position of the receiver. Successive minima are then found by moving the receiver further away from the transmitter and repeating the fine-adjustment procedure. As mentioned earlier, the positions for every other minima are used for the calculations.

Table I shows data for an actual experiment, where the measured frequency of the laser modulation was  $f_m = 434.0094 \pm 0.0002$  MHz. The transmitter is positioned at the zero position of the optical bench, as shown in Fig. 1, and the error on each position measurement  $D_i$  of the transmitter is about 0.5 mm. Only one reading was taken for each position.

In the third column of Table I, the difference between the third and first values of the minimum audio positions is reported, as well as the difference between the fourth and the second. These distances are then used to calculate  $c$  using Eq. (9), reported in the fourth column of Table I, and are then averaged to obtain our final result of  $c = (2.997 \pm 0.003) \times 10^8$  m/s.

### B. Determination of the refraction index of transparent solids and liquids

The receiver is placed in a position of minimum towards the center of the bench. The solid slab or the cell for liquids

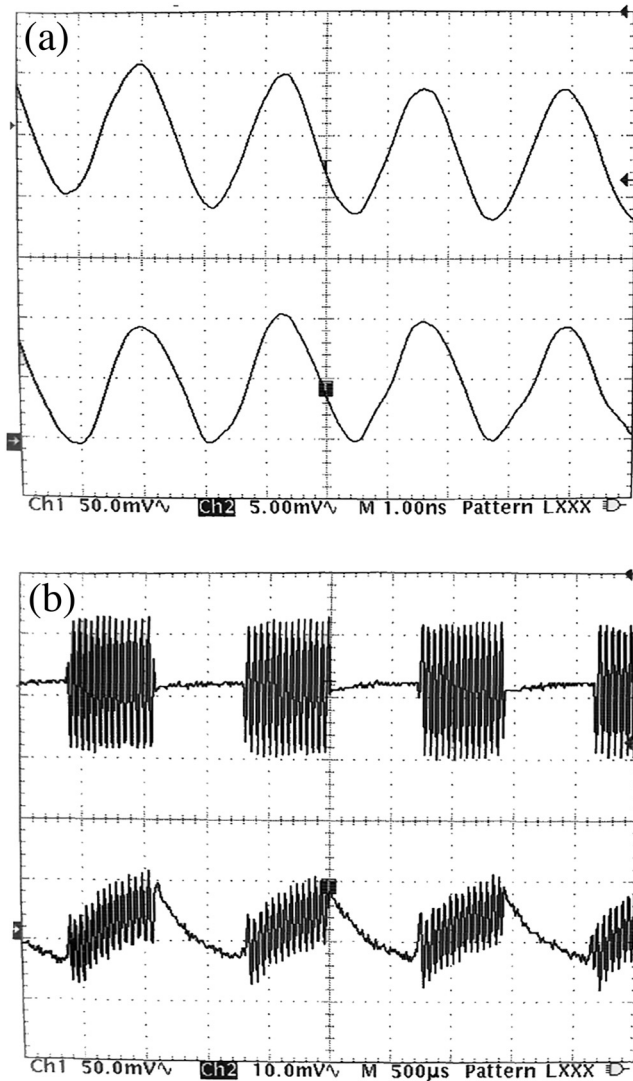


Fig. 10. (a) Oscilloscope screen where the upper trace is the 434 MHz laser modulation signal at 1 ns/div time base, while the lower trace is the photodiode received signal. (b) The same signals are displayed but with a longer horizontal scanning time of 500  $\mu$ s/div. The low frequency ON-OFF modulation of the rf signal and of the laser light is clearly displayed.

is then positioned in the path of the laser beam somewhat close to the receiver, as shown in Fig. 12. It is not necessary for these objects to be aligned with precision, nor for them to have perfectly flat and parallel faces; the light that arrives at the receiver is usually sufficient due to the internal focusing lens. Because the speed of light decreases while passing through the material, to find the new position of the corresponding minimum it is necessary to reduce the distance from the transmitter by  $\Delta D$ . It is easily shown that  $n = 1 + \Delta D/L$ , where  $L$  is the geometrical length that light travels within the material. It is advantageous to perform the measurement on two contiguous minimum positions and average the two  $\Delta D$  values. The instrument is so sensitive that it is even possible to detect the slowing of light passing through the thickness of a microscope slide. Note that the measured result is independent of the value of the rf modulating frequency. With the cell shown in Fig. 12(a) the dependence of  $n$  on the concentration of solutions can be investigated with precision using minimal volumes of liquids.

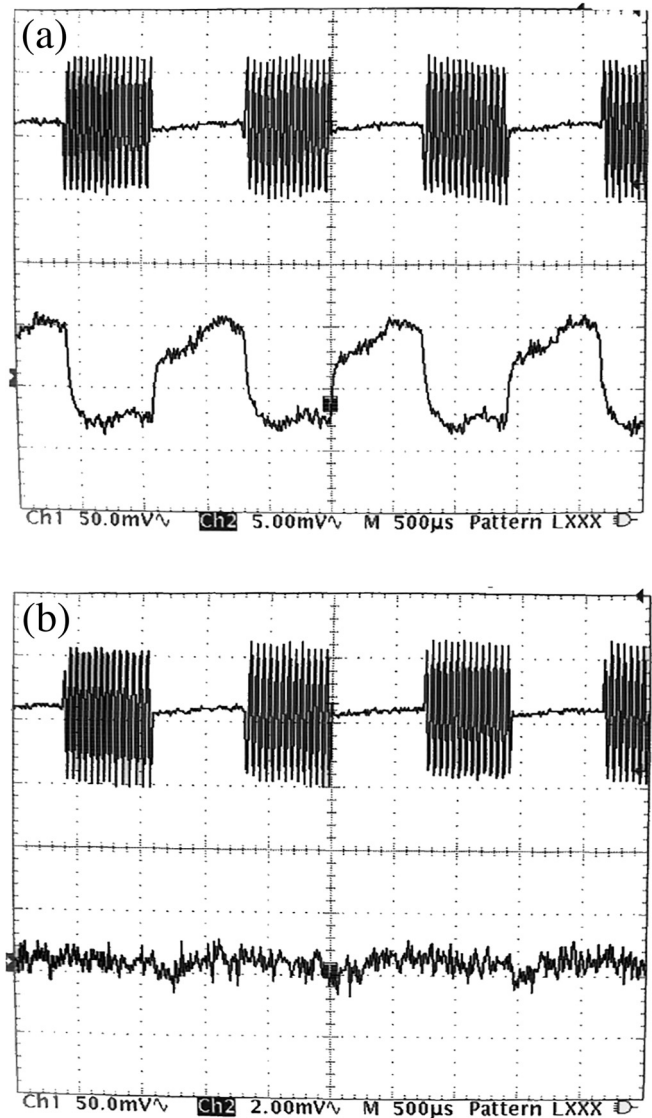


Fig. 11. The upper traces show the rf modulation signal, as in Fig. 10(b), while the lower traces show the signals on the OUT audio connector of Fig. 9. Panel (a) shows a very low audio signal and panel (b) shows a null audio signal when the receiver is positioned at a minimum and only the noise is visible.

### 1. Index of refraction of acrylic

The index of refraction of acrylic was measured by inserting a 10.7 cm-long rod into the beam. The position of a minimum  $D_1$  was found without the rod, along with the new minimum  $D_2$  when the rod was inserted. This procedure was then repeated using an adjacent minimum ( $D_3$  without rod,  $D_4$  with rod), and the results are listed in Table II. The measured index of refraction (with the red laser) was found to be

Table I. Measurements for the determination of  $c$  (the measured modulation frequency was  $f_m = 434.0094 \pm 0.0002$  MHz).

$i$	$D_i$ (cm)	$\Delta D$ (cm)	$c = \Delta D f_m$ ( $10^8$ m/s)	$c_{\text{avg}}$ ( $10^8$ m/s)
1	20.15	...	...	...
2	53.80	...	...	...
3	89.25	69.10 ( $D_3 - D_1$ )	$2.999 \pm 0.002$	...
4	122.85	69.05 ( $D_4 - D_2$ )	$2.996 \pm 0.002$	$2.997 \pm 0.003$

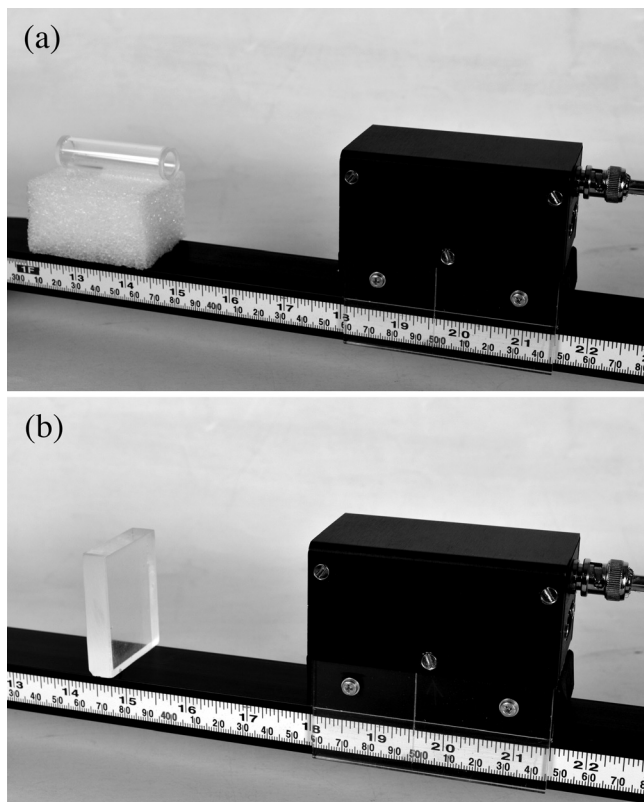


Fig. 12. A cell for liquids (a) and an acrylic glass slab (b) are inserted in the path of the laser-beam.

$n = 1.507$ , while the accepted value (for the yellow sodium line) is  $n = 1.48$ – $1.50$ .

## 2. Index of refraction of water

The index of refraction of water was measured by using a cell containing a 7.65 cm-long column of water. As before, two adjacent minima and their deviations were measured, with the results presented in Table III. The measured index of refraction (with the red laser) was found to be  $n = 1.343$ , while the accepted value (for yellow sodium line) is  $n = 1.33$ . As for the measurement with acrylic, no errors have been reported because only a single measurement was carried out, for demonstration purposes only.

## C. Determination of the velocity factor of a cable

Starting with the receiver in a position of minimum audio signal, the receiver cable is replaced with another longer cable. To find the same minimum, it is necessary to reduce the distance from the transmitter. The velocity of electric signals in the cable is given by  $v = cL/\Delta D$ , where  $L$  is the difference in length between the two cables. Therefore, the

Table II. Measurements for the determination of  $n$  for acrylic.

$i$	$D_i$ (cm)	$\Delta D$ (cm)	$\Delta D_{\text{avg}}$ (cm)	$n = 1 + \Delta D_{\text{avg}}/L$
1	41.90	...	...	...
2	36.05	5.85 ( $D_1 - D_2$ )	...	...
3	79.00	...	...	...
4	74.00	5.00 ( $D_3 - D_4$ )	5.425	1.507

Table III. Measurements for the determination of  $n$  for water.

$i$	$D_i$ (cm)	$\Delta D$ (cm)	$\Delta D_{\text{avg}}$ (cm)	$n = 1 + \Delta D_{\text{avg}}/L$
1	44.60	...	...	...
2	41.70	2.90 ( $D_1 - D_2$ )	...	...
3	82.25	...	...	...
4	79.90	2.35 ( $D_3 - D_4$ )	2.625	1.343

relative permittivity, or dielectric constant, of the insulating material of the cable is  $\epsilon_r = (\Delta D/L)^2$ , where we have assumed the relative magnetic permeability  $\mu_r = 1$ .

The experimental results are shown in Table IV. The original minimum position is denoted  $D_1$  and the new minimum  $D_2$  is determined after replacing the cable with one that is 19.5 m longer (the cable lengths were measured between the connector's ends). As seen in the table, the results show a signal velocity of  $v = 0.670c$  for a normal 50- $\Omega$  cable with a polyethylene insulator, which gives a corresponding relative permittivity of  $\epsilon_r = 2.22$ . For comparison, the accepted value of the dielectric constant of polyethylene is  $\epsilon = 2.25$ .

Incidentally, these results show that a normal coaxial cable, such as the one used here, delays signals by about 1 ns for each 50 cm of its length.

## VI. ADDITIONAL POSSIBILITIES

### A. Doppler frequency shift

As we have previously highlighted, the experimental system described here may be seen as a split beam interferometer working with a carrier frequency of 434 MHz and with one of the signals propagating in free space in one arm while the other propagates along a cable. In this metaphor, the receiver is the moving mirror and the mixer in Fig. 2 acts to recombine the beams.

Equation (4) shows that the output voltage of the mixer of Fig. 2 is the product of two sinusoidal signals of the same amplitude and frequency, one of which delayed in phase by  $\Delta\phi_m$ . When the phase delay is  $0, \pi, 2\pi$  and so on, the two signals have their zeros in coincidence and this corresponds to zero audio signal. If we move the receiver along the optical bench at constant speed, the phase shift varies constantly in time and we hear a succession of maxima and minima of the audio signal. Most important at this point is the following fact. What we hear at the acoustic display is not the  $V_{\text{out}}$  sinusoidally varying signal of Eq. (5), but a coded version of this signal by its further acoustic modulation, at 700 Hz, performed by the laser transmitting circuit of Fig. 5. The detection and amplifier circuit (Fig. 9) cannot distinguish between positive and negative half waves—it gives the absolute value of the output voltage of the mixer—and therefore generates audio output between each successive zero (when the  $\cos \Delta\phi_m$  signal is nonzero), whether positive or negative. The result is that there is a succession of two maxima of the

Table IV. Measurements for the determination of the velocity of a signal through a cable.

$i$	$D_i$ (cm)	$\Delta D$ (cm)	$v/c = L/\Delta D$
1	52.50	...	...
2	23.40	29.10	0.67

audio signal for every  $\lambda$  displacement of the receiver, or every  $2\pi$  rotation of the phase difference. It is interesting to note that the audio signal abruptly changes phase by  $\pi$  when the signal crosses zero, although this fact is inaudible.

For a modulation frequency of  $f_m \approx 434$  Mhz, the succession of two audio maxima every  $\Delta D = c/f_m = 69$  cm corresponds to a single fringe shift in an optical interferometer when one of the mirrors is moved and its optical path has varied by  $\lambda$ . Thus, if  $T$  is the time it takes to move the receiver through one complete fringe, so that  $v = \Delta D/T$ , then the phase shift will vary in time at a frequency  $1/T = f_m v/c$ .

However, this result may also be interpreted as a beating phenomenon between signals with two different frequencies, one at the modulation frequency  $f_m$ , and the other at a Doppler-shifted frequency  $f_D$  that results from the receiver moving toward the source at speed  $v$ .<sup>29</sup> The beat frequency that results from these signals is

$$f_m - f_D = \Delta f_m = \frac{f_m v}{c}, \quad (10)$$

where the right hand side is, neglecting the sign, the Doppler frequency shift for a signal source of frequency  $f_m$  as perceived by a receiver that moves directly toward (or away from) the source with constant velocity  $v$ . (Note that, as explained above, the actual beat frequency you *hear* using the apparatus described here will be twice this frequency.) If we choose a speed  $v = 1.4$  m/s, we find

$$\Delta f_m = 434 \times 10^6 \text{ Hz} \left( \frac{1.4 \text{ m/s}}{3 \times 10^8 \text{ m/s}} \right) \approx 2 \text{ Hz}. \quad (11)$$

This experiment is useful for explaining, for instance, the Doppler corrections performed by a GPS receiver on the time data transmitted by a rapidly moving satellite despite the fact that the speed of the carrier signal is  $\sim c$  and independent of the speed of the satellite.

## B. Fizeau experiment on the partial drag of ether

Because of the compactness and sensitivity of this apparatus, it is well suited for reproducing the Fizeau experiment,<sup>27</sup> originally performed in 1851 on the speed of light in flowing water. In this experiment, Fizeau discovered that the velocity addition rule for light does not correspond to the Galilean rule of velocity addition, and the results appeared to support the partial aether drag hypothesis. Owing to the relatively small values of the speed of flowing water, the Doppler shift explains well the displacement of fringes found by Fizeau and in successive experiments with higher accuracy.

The sensitivity of the apparatus described here is so high that one can use a cell that is only about 20 cm long and water flowing at a relatively slow speed. It is easy to see the difference of the speed of light in flowing water and in still water in a manner that is as simple as the above-described determination of the refraction index of a liquid.

## VII. CONCLUSIONS

In conclusion, we have presented a new advanced apparatus for the determination of the speed of light in free propagation with unprecedented performance. This apparatus facilitates the measurement of several interesting quantities and the experiments can be carried out in a much simpler

manner compared to other apparatuses. The system is compact, autonomous, does not require auxiliary accessories or elements, and is pre-aligned and ready for use in minutes. The apparatus is particularly well suited for use as an exhibit in museums or science centers or as a demonstration from the lecturer's table in conferences or seminars. The working principles of the device can be easily understood by a general audience.

## ACKNOWLEDGMENT

The author gratefully acknowledges Professor G. Torzo of Padua University, Italy, for scientific advice and assistance with editing the manuscript.

- <sup>a)</sup>Electronic mail: pegna@unica.it; Permanent address: Department of Physics, University of Cagliari, Citta Universitaria, 09042 Monserrato (Ca), Italy.
- <sup>1</sup>W. C. Anderson, "A measurement of the velocity of light," *Rev. Sci. Instrum.* **8**, 239–247 (1937).
  - <sup>2</sup>P. F. Hinrichsen and J. C. Crawford, "An improved metrologic speed of light apparatus," *Phys. Teach.* **13**, 504–506 (1975).
  - <sup>3</sup>J. E. Carlsson, "Speed of light measurement with the laser pointer," *Phys. Teach.* **34**, 176–177 (1996).
  - <sup>4</sup>B. Brody, "The speed of light: Making an easy time of it," *Phys. Teach.* **41**, 276–277 (2003).
  - <sup>5</sup>J. Cooke, M. Martin, H. McCartney, and B. Wilf, "Direct determination of the speed of light as a general physics laboratory experiment," *Am. J. Phys.* **36**, 847–848 (1968).
  - <sup>6</sup>C. E. Tyler, "A pedagogical measurement of the velocity of light," *Am. J. Phys.* **37**, 1154–1156 (1969).
  - <sup>7</sup>J. Vanderkooy and M. J. Beccario, "An inexpensive, accurate laboratory determination of the velocity of light," *Am. J. Phys.* **41**, 272–275 (1973).
  - <sup>8</sup>F. D. Becchetti, K. C. Harvey, B. J. Schwartz, and M. L. Shapiro, "Time-of-flight measurement of the speed of light using a laser and a low-voltage Pockels-cell modulator," *Am. J. Phys.* **55**, 632–634 (1987).
  - <sup>9</sup>J. A. Deblaquiere, K. C. Harvey, and A. K. Hermann, "Time-of-flight measurement of the speed of light using an acousto-optic modulator," *Am. J. Phys.* **59**, 443–447 (1991).
  - <sup>10</sup>M. B. James, R. B. Ormond, and A. J. Stasch, "Speed of light measurement for the myriad," *Am. J. Phys.* **67**, 681–684 (1999).
  - <sup>11</sup>K. Aoki and T. Mitsui, "A tabletop experiment for the direct measurement of the speed of light," *Am. J. Phys.* **76**, 812–815 (2008).
  - <sup>12</sup>G. Pegna, "Un esperimento didattico per la determinazione diretta della velocit della luce con il laser," *Giornale di Fisica XVII*(4), 274–279 (1976).
  - <sup>13</sup>G. Brickner, L. A. Kappers, and F. P. Lipschultz, "Determination of the speed of light by measurement of the beat frequency of internal laser modes," *Am. J. Phys.* **47**(12), 1086–1087 (1979).
  - <sup>14</sup>D. J. D'Orazio, M. J. Pearson, J. T. Schultz, D. Sidor, M. W. Best, K. M. Goodfellow, R. E. Scholten, and J. D. White, "Measuring the speed of light using beating longitudinal modes in an open-cavity HeNe laser," *Am. J. Phys.* **78**(5), 524–528 (2010).
  - <sup>15</sup>R. Cohen, H. Goldring, and M. Harrap, "Measuring speed of light with two dollar rotators," *Phys. Teach.* **18**, 226–229 (1980).
  - <sup>16</sup>J. Brody, L. Griffin, and P. Segre, "Measurements of the speed of light in water using Foucault's technique," *Am. J. Phys.* **78**(6), 650–653 (2010).
  - <sup>17</sup>G. Pegna, "Proposta di un metodo per la misura della velocit di un segnale elettrico in un conduttore," *Giornale di Fisica* **14**, 184–186 (1973).
  - <sup>18</sup>Se-Yeuen Mak, "Speed of electromagnetic signal along a coaxial cable," *Phys. Teach.* **41**, 46–49 (2003).
  - <sup>19</sup>All commercial microwave apparatuses in use in undergraduate laboratories allow the interferometric determination of  $c$  by measuring the wavelength of an electromagnetic wave of known frequency. The literature on this subject is very wide; for an example of a precision measurement, see W. Culshaw, "High resolution millimeter wave Fabry-Perot interferometer," *IRE Trans. Microwave Theory Tech.* **MTT** **8**(2), 182–189 (1960).
  - <sup>20</sup>G. Pegna and P. Grosso, "Esperimenti con il Forno a Microonde," *Giornale di Fisica* **46**(3), 183–196 (2005).

- <sup>21</sup>M. C. Schroeder and C. W. Smith, "Estimating the speed of light with a TV set," *Phys. Teach.* **23**, 360 (1985).
- <sup>22</sup>D. Keepports, "Looking for ghosts to measure the speed of light," *Phys. Teach.* **28**, 398–399 (1990).
- <sup>23</sup>J. E. Beaver, "The speed of light with a shortwave radio," *Phys. Teach.* **38**, 172–174 (2000).
- <sup>24</sup>J. Lepak and M. Crescimanno, "Speed of light measurement using ping," e-print [arXiv:physics/0201053](https://arxiv.org/abs/physics/0201053).
- <sup>25</sup>Aurel TX-4MDIL (Farnell code 1699488), with a cost of under [dollar]5. Many other types are available, e.g., on Ebay, as wireless data transmitting modules for Arduino.

- <sup>26</sup>Centronic AEPX65 photodiode (Farnell code 548777).
- <sup>27</sup>H. Fizeau, "Sur les hypotheses relatives a l'ether lumineux," *Comptes Rendus* **33**, 349–355 (1851).
- <sup>28</sup>See supplementary material at <http://dx.doi.org/10.1119/1.4985728> for the Gerber files for the printed circuit boards for the transmitter, receiver, and control unit. Because of the relatively high frequency used, printed circuit boards are recommended for proper functioning of the circuits.
- <sup>29</sup>A somewhat different treatment of the displacement of fringes in an interferometer due to the Doppler effect can be found in D. Malacara, I. Rizo, and A. Morales, "Interferometry and the Doppler Effect," *Appl. Opt.* **8**(8), 1746–1747 (1969).



### Wimshurst Machine

James Wimshurst's design (1882,1883) was based on earlier designs by Holtz, Töpler and Voss. All of these are *influence machines* and operate on the same principle as the electrophorous. This machine, at Hampden-Sydney College, dates from the first quarter of the 20th century, and has an unusual drive mechanism. (Picture and Notes by Thomas B. Green-slade, Jr., Kenyon College)